Journal of the Oceanographical Society of Japan
Vol. 38, pp. 43 to 51, 1982

Numerical Experiment on the Circulation in the Japan Sea
Part I. Formation of the East Korean Warm Current*

Jong-Hwan YOON**

Abstract: By using a rectangular basin of uniform depth with inflow and outflow openings, the circulation in the Japan Sea is investigated numerically. Heat flux through the sea surface is determined from the annual mean atmospheric conditions for the Japan Sea, but no wind stress is considered.

In the transient state, the warm water supplied through an inflow opening travels cyclonically along the coast as a density-driven boundary current in a rotating system. In the quasi-steady state, the warm water flows northward as a western boundary current which corresponds to the East Korean Warm Current and gradually separates from the coast as it flows northward. No strong boundary current corresponding to the nearshore branch of the Tsushima Current exists.

Under annual mean atmospheric conditions, formation of the deep water characteristic of the Japan Sea and of the thermal front corresponding to the Polar Front do not take place.

1. Introduction

The Tsushima Current is a major feature of the hydrography in the Japan Sea, and has a volume transport of about a few percent of that of the Kuroshio. It flows into the Japan Sea through the Tsushima Straits and carries water of high temperature and high salinity toward the north-east. Most of the water flows out through the Tsugaru and Sôya (La Perouse) Straits, and the rest continues to flow along the west side of Sakhalin Island, turns around, and flows southward as the Riman Current after having been cooled and diluted.

Since the Tsushima Current in the Japan Sea shows large variability in flow and its instantaneous flow patterns are very complicated, the mean path of the Tsushim Current has been discussed by many authors. SUDA and HIDAKA (1932) and UDA (1934) proposed that the Tsushima Current is composed of three branches. However, according to TANIOKA (1968) and MORIYASU (1972), it would be appropriate to say that the Tsushima Current is composed of two main branches.

Recently, the Japan Oceanographic Data Center (JODC) summarized and compiled the oceanographic data in the northwestern Pacific Ocean which have been accumulated for about seventy years from 1907–1972 (JODC, 1975, 1978). The annual mean temperature at 100 m (JODC, 1975) is shown in Fig. 1. Clear splitting of the isotherms into two branches can be seen near the Tsushima Straits. The monthly variations

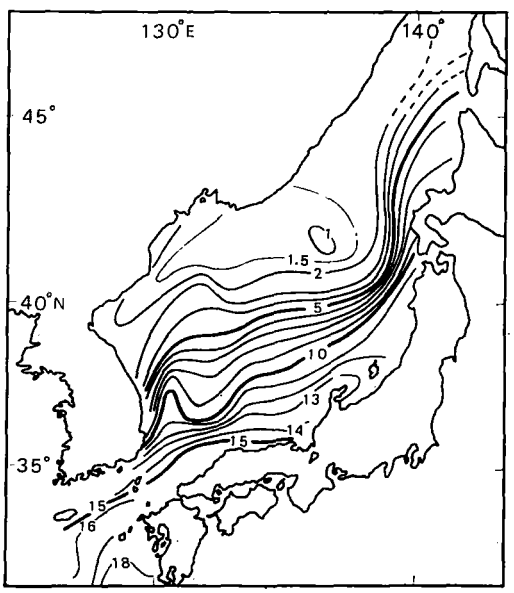

Fig. 1. Annual mean of observed temperature (°C) at a depth of 100 m (JODC, 1975).

* Received Aug. 7, 1981, revised Mar. 4 and accepted Apr. 12, 1982.

** Geophysical Institute, Faculty of Science, University of Tokyo, Bunkyô-ku, Tokyo 113, Japan

of long-term mean temperature at 100 m (JODC, 1978) also show the same splitting of the isotherms near the Tsushima Straits. These temperature data suggest that the Tsushima Current splits into two main branches near the Tsushima Straits. One flows along the Japanese coast as the nearshore branch. The other flows northward along the Korean coast as the East Korean Warm Current. A part of the latter current turns to the south as a counter current and joins the former, while the rest of it flows along the Polar Front, whose position roughly coincides with the isotherm of 6°C in the central region of the Japan Sea. These current branches join west of the Tsugaru Straits. However, no one has provided a physical interpretation of the branching mechanism of the Tsushima Current near the Tsushima Straits.

In the present study and following papers, Parts II (YOON, 1982) and III (YOON, MS), the circulation in the Japan Sea is investigated numerically, focusing attention mainly on the branching mechanism of the Tsushima Current.

YOON and SUGINOHARA (1977) studied numerically the behavior of the warm water flowing into a cold ocean. The warm water supplied through a southern opening was found to travel in two directions: that is, the warm water travels both eastwards and westwards along the southern coast. The eastward traveling speed of warm water along the southern boundary as a density-driven boundary current is much faster than the westward traveling speed of warm water. Since this behavior of warm water is transient, it seems to be necessary to investigate the behavior of the warm water flowing into the ocean in a steady state. However, since a long-time integration is needed to attain the steady state, a quasi-steady state is considered in the present study.

The present study (Part I) is intended to determine whether a strong boundary current can exist or not as a density-driven boundary current in a quasi-steady state, and whether or not the formation of the front corresponding to the Polar Front takes place in the quasi-steady state under annual mean atmospheric conditions in the Japan Sea.

2. Model

A rectangular coordinate system on a β-plane is used, taking x eastward, y northward, and z upward from mean sea level ($z=0$). The equations of motion (the primitive equations) are simplified by making the Boussinesq and hydrostatic approximations and by assuming an equation of state of the form

$$\rho=\rho_0(1-\alpha T) \qquad (1)$$

where ρ is the density, T is the temperature, $\alpha=0.0002/°C$ is the coefficient of thermal expansion and $\rho_0=1\,\mathrm{g\,cm^{-3}}$. The coefficients of horizontal (A_h) and vertical (A_v) eddy viscosity, and thermal diffusivity (K) are assumed to have constant values

$$A_h=K_h=10^7\mathrm{cm^2\,s^{-1}},\quad A_v=K_v=0.5\,\mathrm{cm^2\,s^{-1}}.$$

A schematic view of the model ocean (shown in Fig. 2) is regular square box with sides of 900 km and a depth of 2,000 m. The model ocean has two openings: one is at the southern wall and the other at the eastern wall. The southern opening with a width of 180 km and a depth of 110 m corresponds to the Tsushima Straits. The eastern opening with a width of 60 km and a depth of 110 m corresponds to the Tsugaru Straits. In a horizontal plane 15×15 grid points are spaced at regular intervals of 60 km. Since the Munk's width of the western boundary layer $L_M=2\pi/\sqrt{3}(A_h/\beta)^{1/3}$ is 134 km for the value of $\beta(2\times10^{-13}\,\mathrm{s^{-1}\,cm^{-1}})$, this grid interval is fine enough to resolve the viscous western boundary layer. In the vertical plane there are 9 layers as shown in Table 1.

Table 1. Thickness of each layer.

Layer	1st	2nd	3rd	4th	5th	6th	7th	8th	9th
Thickness (m)	20	20	30	40	60	120	240	480	990

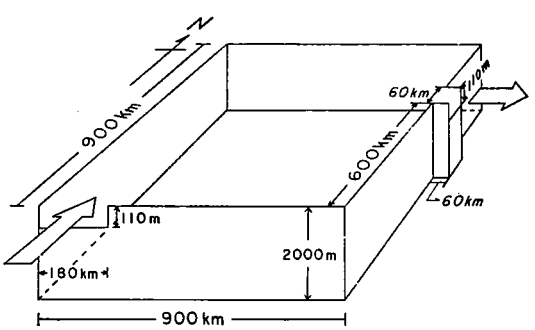

Fig. 2. Schematic view of the model ocean.

Motion is forced at the southern opening by imposing a mass and heat flux, and at the ocean surface by imposing a thermal flux. These boundary conditions are described in the following sections. At the vertical wall each of the velocity components and the heat flux are zero. The ocean floor is stress free and adiabatic. The numerical scheme is basically the same as that in BRYAN (1969).

3. Conditions of inflow and outflow

The vertical distributions of temperature and northward velocity prescribed at the inflow opening are shown in Table 2. These values do not vary horizontally within the opening and are fixed throughout the calculation. The distribution of temperature is determined on the monthly mean vertical sections of temperature in the Tsushima Straits reported by NAN'NITI and FUJIKI (1967). From the velocity distribution in Table 2, the total volume transport through the inflow opening is estimated as 2.16×10^{12} cm^3 s^{-1}. The slippery condition for the zonal component of the velocity at this opening is adopted.

The boundary condition at the outflow opening may be written as

$$v_x=T_x=0 \qquad (2)$$

and

$$u=u_a+A, \qquad (3)$$

where u_a is the eastward velocity on the adjacent interior grid point. Since the outflow opening has only one grid point, the constant value A is determined so as to equate the volume transport through the opening to that through the inflow opening:

$$A=\frac{V_I}{hl}-\frac{1}{h}\int_{-h}^{0}u_a dz \qquad (4)$$

Table 2. Vertical distribution of the temperature and northward velocity prescribed at the inflow opening.

Layer	Thickness (m)	Temperature (°C)	Northward velocity (cm s^{-1})
1st	20	19	20
2nd	20	18	15
3rd	30	17	10
4th	40	16	5

where h and l are the depth (110 m) and the width (60 km) of the outflow opening, respectively. The constant V_I which is the volume transport through the outflow opening is taken to have the same value as that through the inflow opening.

4. Thermal boundary conditions at the sea surface

The formulation of thermal boundary conditions at the sea surface is similar to that described by HANEY (1971). The net downward heat flux across the ocean surface is given by the sum of the downward flux of solar radiation Q_S, minus the upward flux of longwave radiation Q_B, sensible heat flux Q_H, and latent heat flux Q_E. If the net downward heat flux is denoted by Q_N, we have

$$Q_N=Q_S-(Q_B+Q_H+Q_E). \qquad (5)$$

The downward flux of solar radiation per unit area is calculated by Ångstrom's empirical formula, i.e.,

$$Q_S=Q_{SO}(1-0.71\,n_C)\,(1-\alpha_G), \qquad (6)$$

where Q_{SO} is the amount of the solar radiation which strikes the ocean surface through a cloudless atmosphere, n_C is the cloud amount in decimal form, and α_G, the albedo of the ocean surface, is taken to have a constant value of 0.07. The net upward flux of longwave radiation Q_B is approximated by the following empirical relationship presented by KRAUS and ROOTH (1961):

$$Q_B(T_S)=Q^*\sigma T_S^4, \qquad (7)$$

where

$$Q^*=0.985[0.39-0.05(e_A)^{1/2}]\,(1-0.6\,n_C^2) \qquad (8)$$

and σ is the Stefan-Boltzmann constant, T_S is the ocean surface temperature (°K), and e_A is the vapor pressure (mb) of the air 10 m above sea level. The vapor pressure e_A is given by the following formula (see FLEAGLE and BUSINGER, 1963: pp. 62-63):

$$e_A=re_S(T_A)=r\times10^{(9.4051-2353/T_A)} \qquad (9)$$

where r is the relative humidity in decimal form and $e_S(T_A)$ is the saturation vapor pressure at the air temperature T_A 10 m above sea level.

The upward flux of sensible and latent heat in terms of T_S and the prescribed atmospheric parameters are as follows:

$$Q_H(T_S)=\rho_A C_D V_A C_p(T_S-T_A), \quad (10)$$

$$Q_E(T_S)=\rho_A C_D V_A L[q_S(T_S)-q_A(T_A)] \quad (11)$$

where ρ_A is the air density, C_p the specific heat of air at constant pressure, C_D the drag coefficient, V_A the wind speed (cm s^{-1}), L the latent heat of vaporization, $q_S(T_S)$ the saturation specific humidity at the temperature of the ocean surface T_S, and $q_A(T_A)$ the specific humidity of the air at the 10-m level. The variable drag coefficient proposed by DEACON and WEBB (1962) for neutral stability is employed:

$$C_D=(1.0+0.0007V_A)10^{-3}. \quad (12)$$

Quantities q_S and q_A are represented as follows:

$$q_S(T)=\frac{0.622}{P_A}e_S(T), \quad (13)$$

$$q_A(T)=\frac{0.622}{P_A}e_A(T). \quad (14)$$

The following constant values are used

$$\rho_A=1.2\times10^{-3}\ \text{g cm}^{-3}$$
$$L=595\ \text{Cal g}^{-1}$$
$$C_p=0.24\ \text{Cal g}^{-1}(^\circ\text{C})^{-1}$$
$$P_A=1013.25\ \text{mb}.$$

In the present model, the ocean surface temperature T_S is replaced with temperature T_1 at the first level below the ocean surface.

Annual mean meteorological elements T_A, r, n_C, V_A and Q_{SO} used in this model are shown in Fig. 3. The first four elements are obtained by taking the annual average of the monthly mean data reported by the MAIZURU MARINE OBSERVATORY (1972), and the last element is calculated from the monthly mean data obtained as a function of latitude by BUDYKO (1974: pp. 1-11).

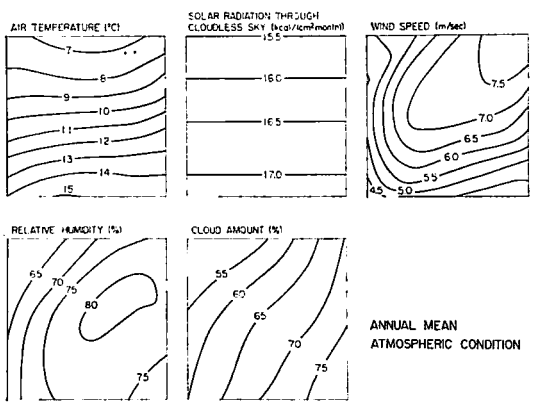

Fig. 3. Annual mean atmospheric elements.

5. Results

In the initial state, the ocean is filled with 1°C water corresponding to the Proper Water in the Japan Sea. The initial velocity fields in the interior of the ocean are somewhat artificial: the northward flow imposed on the inflow opening continues to flow northward until it reaches the latitude of the outflow opening, then it changes direction eastward and flows out through the outflow opening. Time integration is carried out for 2,270 days. The averaged total kinetic energy per unit area and the temperature horizontally averaged at each level are shown in Fig. 4. The total kinetic energy has already become steady by the 1,200th day. Temperatures of the upper 5 levels have become quasi-steady by the 2,270th day, while those of the lower 4 levels are still increasing.

Initially the warm water supplied into the

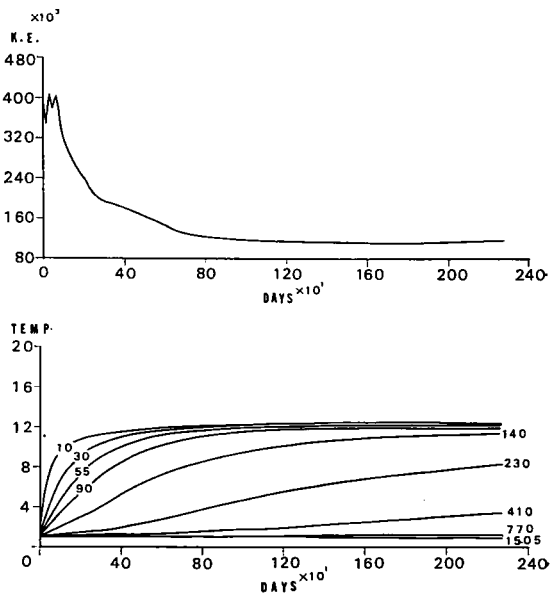

Fig. 4. Time change of the averaged total kinetic energy per unit area (erg cm^{-2}) (upper); and the time change of the horizontally averaged temperature (°C) at each level (m) (lower).

ocean travels cyclonically along the boundary as a density-driven current as shown in Fig. 5 which indicates the instantaneous patterns of the velocity fields at transient stages (15th and 75th days). The travelling speed (U_D) and the width of the forefront are about 25 cm s^{-1} and 100 km respectively. The width of the boundary current behind the forefront increases with time. The reason for this movement with the coast to the right was explained qualitatively by YOON and SUGINOHARA (1977). This stage is characterized by the time scale $T_D=4L/U_D$ (L is the horizontal scale of the basin). In the time $T_D\approx 170$ days ($L=900$ km and $U_D=25$ cm s^{-1}) this boundary current travels around the basin.

Due to the β-effect and the reduction of density difference between the inflowing and interior water, this boundary current weakens and separates from the eastern boundary, and finally disappears. The time scale for a quasi-steady state is roughly $T_R=L/C_R$ (C_R is the phase velocity of the internal Rossby wave). By using the stratification in Fig. 7, T_R is calculated to be the order of 1,000 days.

Fig. 6 shows the horizontal temperature and velocity fields at depths of 10 and 90 m in a quasi-steady state (2,270th day). In the quasi-steady state the transient boundary current traveling cyclonically along the coast disappears and a strong western boundary current is formed. This northward western boundary current gradually separates from the coast as it flows northward, forming a broad eastward flow that converges toward the outflow opening. The width and the maximum velocity of the western boundary current at 90 m are about 100 km and 12 cm s^{-1}, respectively. The directions of the isotherms at 10 m are similar to those of air temperature, although the water temperatures are a few degrees warmer than those of the air temperature (see Fig. 3). At a depth of 90 m, the directions of the isotherms are also similar to those of the air temperature everywhere, except in the southern portion of the western boundary where a large horizontal temperature gradient appears associated with the western boundary current. The resemblance between upper layer temperature and air temperature indicates the strong constraint of atmospheric conditions on the upper layer velocity field. If there is no heat flux through the sea surface, the current system in the upper layer will be largely affected by the β-effect, and the western boundary current confined in the Munk layer L_M will flow straight northward until it reaches the latitude of the outflow opening and then turns to the right and flows out through the outflow opening. But, because of the presence of atmospheric conditions, the western boundary current feeds the broad surface eastward flow induced by the atmospheric conditions imposed at the sea surface. This suggests that both atmospheric conditions and the latitude of the outflow opening are important in the separation of the East Korean Warm Current. The reasons for the disappearance of the boundary current along the

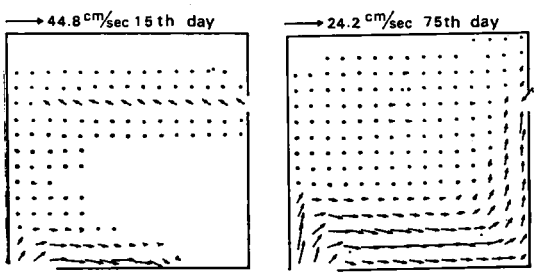

Fig. 5. Horizontal velocity fields at a depth of 10 m on the 15th and 75th day.

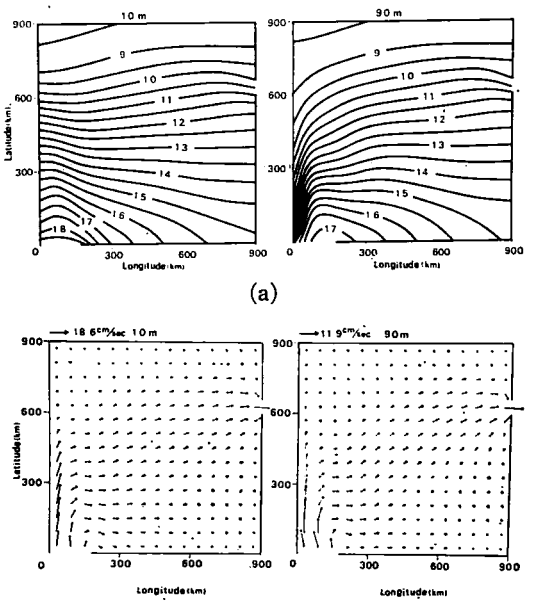

Fig. 6. Horizontal temperature (°C) fields (a) and velocity field (b) at depths of 10 m and 90 m on the 2,270th day.

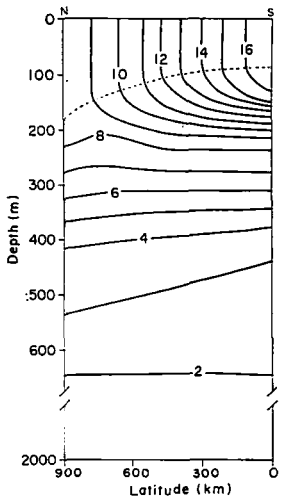

Fig. 7. North-south vertical section of the temperature field (°C) at $x=360$ km on the 2,270th day. The dashed line indicates the depth of the thermal mixed layer.

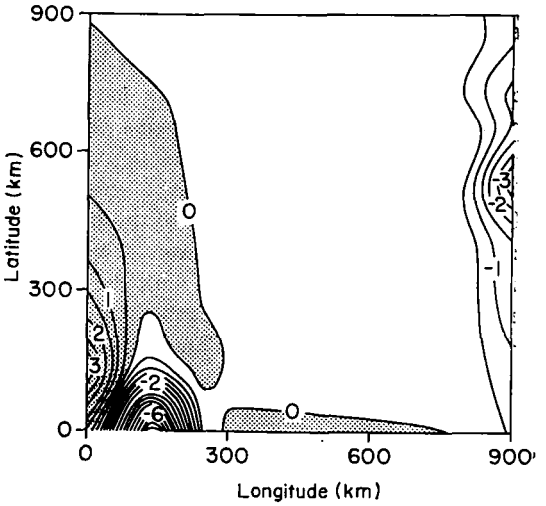

Fig. 8. Horizontal distribution of vertical velocity (10^{-3} cm s^{-1}) at a depth of 70 m on the 2,270th day. The shaded areas are upwelling regions.

south and east coasts are the reduction of temperature difference between the inflowing and the interior waters, as well as the β-effect.

Fig. 7 shows a north-south vertical section of the temperature field at $x=360$ km. The dashed line indicates the depth of the lower boundary of the thermal mixed layer, which is formed by convective adjustment. It does not reach the bottom; i.e., the formation of the deep water which corresponds to the Proper Water in the Japan Sea does not take place anywhere in the present model. In addition, the Subarctic Water, whose temperature at 100 m is 1°~2°C according to observations, is not formed. There are no strong thermal fronts corresponding to the front of the nearshore branch of the Tsushima Current or the Polar Front which is a boundary surface between the Subarctic Water and the Tsushima Warm Water. However, a very weak thermal front with an index temperature of 12°C exists at the position corresponding to the position of the Polar Front. If the atmospheric condition showed the seasonal variation, this weak front might be greatly intensified. Fig. 8 shows the horizontal distribution of the vertical velocity at a depth of 70 m. In the case of a purely thermal circulation without rotation and inflow, it might be expected that flow would be directed down the pressure gradient. With the atmospheric boundary conditions used in these calculations the result would be a meridional circulation with rising motion at low latitudes and northward movement at the surface. The effect of rotation is to induce flow along lines of constant pressure rather than across them. The surface temperature gradient imposed by the atmospheric conditions forces an eastward geostrophic flow. Continuity requires an upward motion near the western boundary and a downward motion near the eastern boundary to balance this surface flow induced by the surface thermal atmospheric conditions.

This mechanism explains the weak vertical motion ($<10^{-3}$ cm s^{-1}) along the western and eastern boundary. But the strong upward motion ($>10^{-3}$ cm s^{-1}) attached to the western boundary current remains to be explained. This latter upward motion is very interesting in relation to the appearance of cold water in the East Korean Warm Current region along the Korean coast (TANIOKA, 1968; AN, 1974).

The total heat flux into the model ocean is given by the sum of the net downward heat flux across the ocean surface and the heat fluxes by advection through the two openings. The heat fluxes through the inflow opening and the outflow opening denoted by Q_{v1} and Q_{v2} respectively are defined by

$$Q_{v1}=C_{pw}\rho_0\iint_{S_1} T_1 v_1 dS \qquad (15a)$$

$$Q_{v2}=C_{pw}\rho_0\iint_{S_2}T_2v_2dS \qquad (15b)$$

where C_{pw} ($=0.934$ cal g^{-1}), ρ_0, T, v are the specific heat of sea water at constant pressure, the mean density, the temperature at the opening, and the velocity* normal to the opening surface S respectively. The subscripts 1, 2, refer to the inflow and outflow openings.

If the total heat flux into the model ocean is denoted by Q, we have

$$Q=\iint_{\Gamma}Q_N d\Gamma+Q_{v1}+Q_{v2} \qquad (16)$$

where the net downward heat flux per unit area Q_N is defined by Eq. (5) and Γ is the model ocean surface. Figure 9 shows the net downward heat flux Q_N across the ocean surface. The large heat flux region is located in the western boundary region where the strong western boundary current intersects the isotherms at large angles (>90°), and so heat advection is strong. The total amount of the net downward heat flux across the ocean surface is -70.7×10^{16} cal d^{-1}. From the distributions of temperature and velocity at the openings which are shown in Tables 2, 3 Q_{v1} and Q_{v2} are calculated to be 309.4×10^{16} and -173.1×10^{16} cal d^{-1}, respectively. Hence, the total heat flux into the model ocean is 65.6×10^{16} cal d^{-1}. This heat flux Q warms the water at a rate on the order of a few degrees per 10 years in the deep layer (>300 m), where the average temperature does not become steady in the present experiment.

Table 3. Vertical distribution of the calculated temperature and eastward velocity at the outflow opening on the 2,270th day.

Layer	Thickness (m)	Temperature (°C)	Eastward velocity (cm s^{-1})
1st	20	10.33	34.60
2nd	20	10.13	33.87
3rd	30	9.90	32.84
4th	40	9.62	31.14

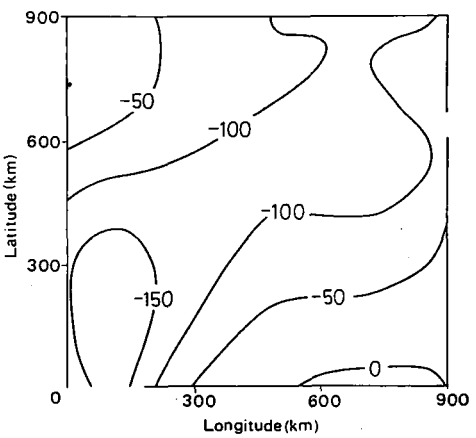

Fig. 9. Net downward heat flux (1y d^{-1}) across the model ocean surface on the 2,270th day.

* Inflow direction is taken to be positive.

To obtain a complete steady state in this model, the time integration must be carried out for the thermal relaxation time H^2/K_v (~3,000 years), where H is the depth of the model ocean. In a complete steady state, the temperature of the deep water will be determined by the temperature T_1 at the first level in the northern portion of the model ocean, where the formation of the deep water will take place. The temperature T_1 at the steady state will not differ so much from that on the 2,270th day. In the steady state, the heat flux across the ocean surface and through the outflow opening must be compensated by the heat flux through the inflow opening. If the temperature T_1 becomes about 1°C warmer than that on the 2,270th day uniformly all over the upper few levels, the total net heat flux across the model ocean surface and the heat flux through the outflow opening will be 118.8×10^{16} cal d^{-1} and about 190.0×10^{16} cal d^{-1}, respectively. The sum of these values will be large enough to compensate the heat flux through the inflow opening. From the above, it seems appropriate to say that the characteristic features in the upper layer (<140 m depth) in a quasi-steady state will not differ so much from those in a complete steady state, although those of the deep layer will vary greatly.

6. Summary and discussion

A quasi-steady state evolves as follows after the sudden input of warm water through the inflow opening. In the initial stage ($t<T_D$) the inflowing warm water travels cyclonically along the coast as a density-driven current. During

the transient period ($T_D<t<T_R$) this density-driven boundary current disappears and a quasi-steady state ($t>T_R$) is obtained. In the quasi-steady state, only a western boundary current exists which separates gradually from the western boundary.

Under annual mean atmospheric conditions, the formation of the deep water does not take place. Therefore, the sharp thermal front corresponding to the Polar Front, which is a boundary between the Subarctic Water and the Tsushima Warm Water, does not form.

The seasonal variation of atmospheric forcing or the effect of the continental shelf might be necessary to maintain the nearshore branch in a steady state. Severe winter-time cooling will produce cold water effectively and might maintain a big density difference between inflowing and interior water, which is favorable for the existence of the density-driven current. The presence of bottom topography is another factor favorable for the formation of the current flowing along the Japanese coast since it provides a strong constraint against the current path due to the effects of ambient potential vorticity. In the following two papers, these effects will be examined.

Acknowledgements

The author expresses his hearty thanks to the late Professor Kozo YOSHIDA for his guidance and encouragement during this work.

References

AN, H.S. (1974): On the cold water mass around the southeast of Korean Peninsula. J. Oceanol. Soc. Korea, **9**, 10-18.

BRYAN, K. (1969): A numerical method for the study of the circulation of the world ocean. J. Comp. Phys., **4**, 347-376.

BUDYKO, M.L. (1974): Climate and Life, Academic Press, New York, 508 pp.

DEACON, E.L. and E.K. WEBB (1962): Interchange of properties between sea and air. *In*, The Sea: Vol. 1. ed. by H. U. SVERDRUP, M. W. JOHNSON and R. H. FLEMING, Wiley Interscience, New York, pp. 49-87.

FLEAGLE, R.G. and J.A. BUSINGER (1963): An Introduction to Atmospheric Physics. Academic Press, New York, 346 pp.

HANEY, R.L. (1971): Surface thermal boundary condition for ocean circulation model. J. Phys. Oceanogr., **1**, 241-248.

JAPAN OCEANOGRAPHIC DATA CENTER [JODC] (1975): Marine Environment Atlas: Northwestern Pacific Ocean I (annual mean). Japan Hydrogr. Association, Tokyo, 164 pp.

JAPAN OCEANOGRAPHIC DATA CENTER [JODC] (1978): Marine Environment Atlas, Northwestern Pacific Ocean II (seasonal and monthly). Japan Hydrogr. Association, Tokyo, 157 pp.

KRAUS, E.B. and C. ROOTH (1961): Temperature and steady state vertical heat flux in the ocean surface layers. Tellus, **13**, 231-238.

MAIZURU MARINE OBSERVATORY (1972): Marine meteorological Study of the Japan Sea. Tech. Rep. Japan Marit. Agency, (8), 1-116.

MORIYASU, S. (1972): The Tsushima Current. *In*, Kuroshio, Its Physical Aspects. ed. by H. STOMMEL and K. YOSHIDA, Univ. of Tokyo Press, Tokyo, pp. 353-369.

NAN'NITI, T. and A. FUJIKI (1967): Secular variations of hydrographic conditions in the East Tsushima Strait. J. Oceanogr. Soc. Japan, **23**, 201-212 (in Japanese).

SUDA, K. and K. HIDAKA (1932): The results of the oceanographical observations on board R.M.S. "Syumpû Maru" in the southern part of the Japan Sea in the summer of 1929, Part I. J. Oceanogr. Imp. Mar. Observ., **3**, 291-375 (in Japanese).

TANIOKA, K. (1968): On the Eastern Korea Warm Current (Tōsen Warm Current). Oceanogr. Mag., **20**, 31-38.

UDA, M. (1934): The results of simultaneous oceanographical investigations in the Japan Sea and its adjacent waters in May and June 1932. J. Imp. Fisher. Exp. St., **5**, 57-190 (in Japanese).

YOON, J.H. (1982): Numerical experiment of the Japan Sea. Part II: Influence of the seasonal variations of atmospheric conditions on the Tsushima Current. J. Oceanogr. Soc. Japan, **38**, 81-94.

YOON, J.H. (MS): Numerical experiment of the Japan Sea. Part III: Formation of the nearshore branch of the Tsushima Current. J. Oceanogr. Soc. Japan, **38**(3) (in press).

YOON, J.H. and SUGINOHARA (1977): Behavior of warm water flowing into a cold ocean. J. Oceanogr. Soc. Japan, **33**, 272-282.

日本海の海洋循環についての数値実験
I. 東鮮暖流の形成

尹　　宗　煥*

要旨: 流入，流出口を持つ，深さ一定の矩形の海のモデルを用いて，日本海における海洋循環の数値実験を行った．海表面における気象条件としては，年平均された気象要素を用いた．南の流入口から供給された暖水は過渡期においては密度流として沿岸に沿って反時計回りに流れるが，準定常状態では，この密度流が消滅し対島海流の沿岸分枝に相当するような境界流は形成されず，西岸に沿って流れる西岸強化流（東鮮暖流）のみが現われるが，それは北上するに従って漸次に陸岸から離れる．また年平均の気象条件のもとでは日本海固有水や極前線は形成されない．

* 東京大学理学部地球物理学教室
〒113 東京都文京区弥生 2-11-16